

Scaled Eagle Nebula Experiments on NIF
DE-SC0008661

Marc W. Pound
University of Maryland

March 28, 2017

Summary

We performed scaled laboratory experiments at the National Ignition Facility laser to assess models for the creation of pillar structures in star-forming clouds of molecular hydrogen, in particular the famous Pillars of the Eagle Nebula (Figure 1). Because pillars typically point towards nearby bright ultraviolet stars, sustained directional illumination appears to be critical to pillar formation. The experiments mock up illumination from a cluster of ultraviolet-emitting stars, using a novel long duration (30–60 ns), directional, laser-driven x-ray source consisting of multiple radiation cavities illuminated in series. Our pillar models are assessed using the morphology of the Eagle Pillars observed with the Hubble Space Telescope, and measurements of column density and velocity in Eagle Pillar II obtained at the BIMA and CARMA millimeter wave facilities. We assess a shielding model for pillar formation. The experimental data suggest that a ‘shielding pillar’ can match the observed morphology of Eagle Pillar II, and the observed Pillar II column density and velocity, if augmented by late time cometary growth.



Figure 1: Molecular pillars like those of the Eagle are examples of a phenomenon that is commonly seen wherever molecular clouds are situated nears O stars: large “fingers” of gas and dust that point directly back at the highly energetic young stars. The middle pillar of Eagle is commonly referred to as “Pillar II.”

Software Development

Astrophysical Radiative Hydrodynamic Simulations

Figure 2 shows two simulations of a shielding model of Eagle Pillar II that using astrophysical code we developed (Kane et al. 2015). The initial condition is a cylindrically symmetric background cloud several pc in radius and 1 pc long. The cloud contains a massive core near the surface of the cloud closest to the star illuminating the cloud. Initial conditions in actual molecular clouds are unlikely to be this simple. Molecular clouds are filamentary, clumpy and turbulent due to gravitational collapse, cooling, and processing by shock waves. However, the static initial conditions used in our simulation lead to a pillar morphologically similar to the central pillar (Pillar II) of the Eagle Nebula, with column density and velocity profiles similar to those observed by BIMA and CARMA. These simplified initial conditions are also feasible for imitation scaled laboratory astrophysics experiments.

In the shielding model, a dense clump in a background cloud protects a column of cold material from the stellar source. As the source turns on, the UV radiation is absorbed in a thin layer cloud at the illuminated cloud surface. In the simulations, material is photoevaporated from the surface, creating a low density, $n_H = 10^2 - 10^3 \text{ cm}^{-3}$, $\sim 20 \text{ km s}^{-1}$ outflow perpendicular to the surface. In reaction, a $\sim 9 \text{ km s}^{-1}$ shock is driven into the cloud. Unshielded cloud material is shock-compressed past the clump, while the shock passes more slowly through the denser clump, at $\sim 3 \text{ km s}^{-1}$, which therefore remains essentially stationary. The result of this differential compression is a pillar of background cloud material exposed behind the clump. The dynamics are somewhat more involved, however. The shock also wraps around behind the clump, laterally compressing the shielded material towards the axis of the pillar, and also giving the compressed material a velocity component along the axis of the pillar, away from the clump. Thus, eventually leads to a shocked clump separated from a shocked, receding cloud. However, at later times, material that is photoevaporated from the clump, or released when the shock exits the clump, also collects behind the clump, creating a second, late-time source of material for the pillar. This process of the clump releasing material downstream is the beginning of the formation of a secondary, ‘cometary’ structure. The compressed, pressurized material on the axis is also able to rebound off the axis, and the converging transverse shocks reflect from the axis.

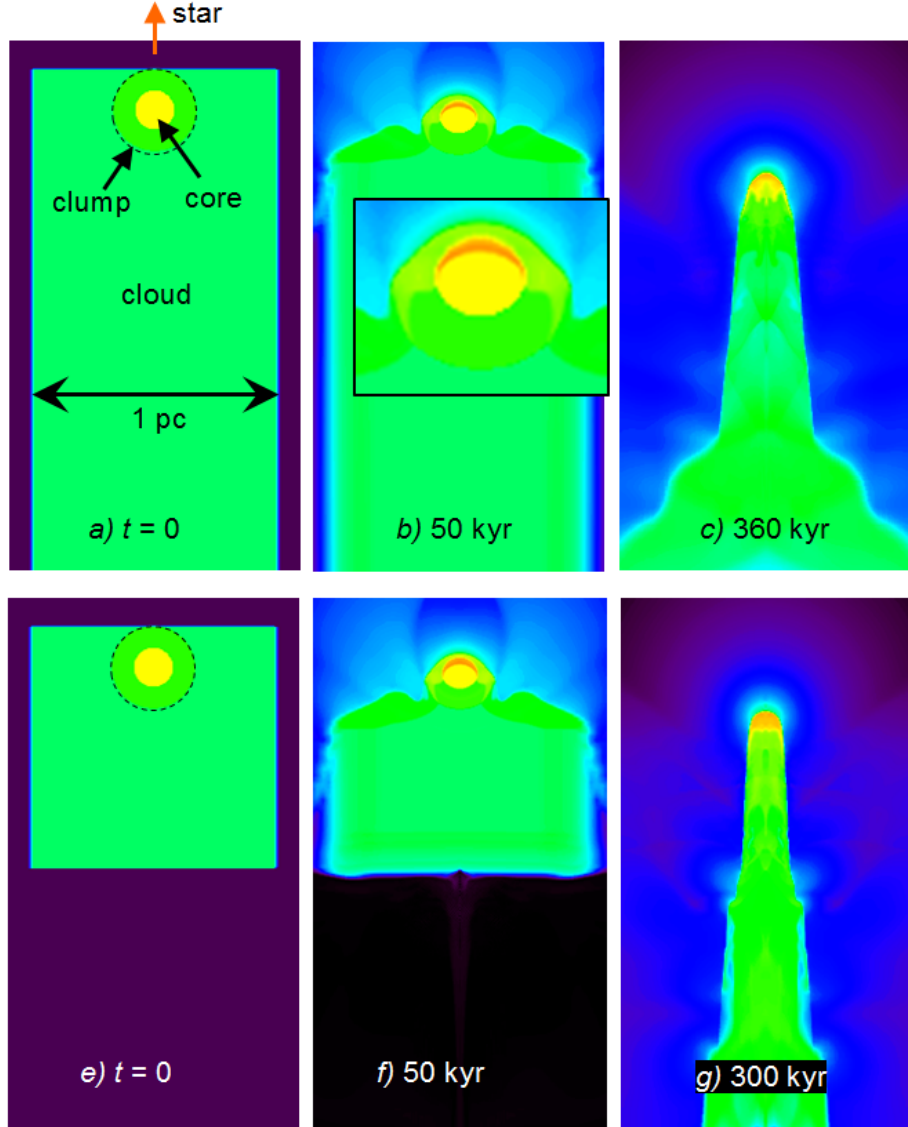


Figure 2: Astrophysical simulations of Eagle Pillar II. a): An initial cloud containing a clump with a dense core is located 1.5 pc from a bright O-type star. b) UV Radiation from the star photoevaporates the outer surface of the cloud, driving a shock into the cloud, and more slowly into the clump and core (inset), c) exposing a pillar of shielded material. d) With an assumed tilt angle of 35° out of the plane, the projected column density and the velocity gradients are similar to the Pillar II profiles observed at BIMA and CARMA. The deficit of column density in the middle of the pillar suggests the initial shielded pillar dissipates. e)-g) A shorter initial cloud evolves into a longer, better connected column with a cometary component filling in the density deficit, g) matching the millimeter wave data better.

Synthetic Observations

We developed software to create "synthetic observations" of our radiative hydrodynamic simulations that can be directly compared to our mm-wave interferometric observations (using the BIMA and CARMA interferometers), allowing us to assess the best match of various initial/final conditions in the astrophysical models. Briefly, the process is as follows.

The 2D cylindrically symmetric simulation outputs from our astrophysical code are converted to 3D by rotating them around the central axis and reproducing them every 0.5 degrees, and adding that to a summed model, in this way building up the full 3D cube. This method keeps the full x, y, z, v_x, v_y, v_z and computes mass per cell. The 3D models are then inclined by $i = 20, 25, 30, 35$ degrees with respect to vertical, moving the tail away from the observer as in Eagle Pillar II; in the process recomputing quantities like observed radial velocity and mass along each line of sight.

Each of these inclined models is rotated by position angle 129 degrees in the plane of the sky and placed at a distance of 1900 pc to match the RA,DEC orientation and distance of Eagle Pillar II. All other coordinate headers are matched with the Eagle mm-wave interferometer observations and rebinned velocity to match the CO data sampling (0.25 km/s). From these we create u - v visibility data by sampling each model with the interferometer Fourier coverage and primary beam pattern, adding Gaussian noise comparable in scale to the CO data. The visibilities are then Fourier Transformed and deconvolved with the same methods used for the original CO data. The output is a simulated observation data cube that is directly comparable with the astronomical data cube.

From the data cubes, we create position-velocity slice and emission weighted moment maps (moment 0 is integrated intensity, moment 1 is mean velocity, moment 2 is velocity dispersion; see <http://www.astro.umd.edu/mpound/eaglenif>) We further create the emission-weighted velocity plots by weighted averaging the position-velocity slices along the velocity axis. An example is shown in Figure 3.

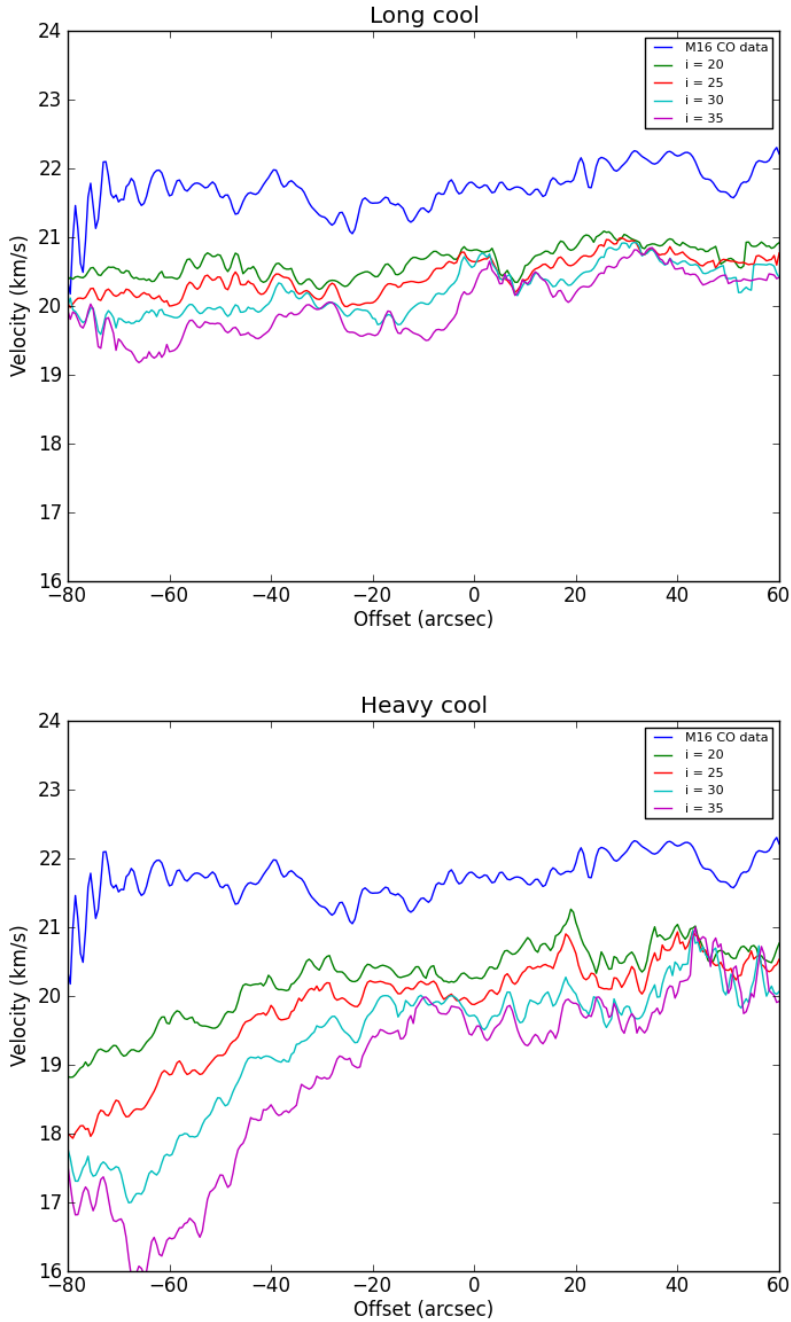


Figure 3: Emission-weighted velocity derived from CO astronomical observations of Pillar II (“M16 CO data”) and from two sets of our radiative hydrodynamic models for various inclination angles i to the line of sight. The pillar head is at positive Offset, the tail at negative offset. The velocity of the CO data is offset for easier comparison with the models: what matters here is the overall shape of the curves—the relative velocities of head and tail. The bottom panel results from a spherical, very massive initial molecular core. In this model, the tail velocities drop off sharply, unlike the observed CO data. The top panel represents a less massive initial core with a lengthwise extension (e.g. Figure 2e-g). In this case, the head-to-tail relative velocities match better the CO data.

NIF Experiments

NIF is a 192 beam laser capable of delivering up to 2 MJ of $0.35\text{ }\mu\text{m}$ laser energy to a mm-scale target, on time scales of 1 ns to 10s of ns. Laser-driven hydrodynamics experiments typically use drives lasting up 15 ns. For our purpose of creating a large (millimeter scale), ablatively confined structure, we require a sustained drive lasting 30 to 60 ns, which is long by the standards of laser experiments. Figure 4 shows the new laser-driven x-ray source we developed to produce such long drives in our NIF experiments.

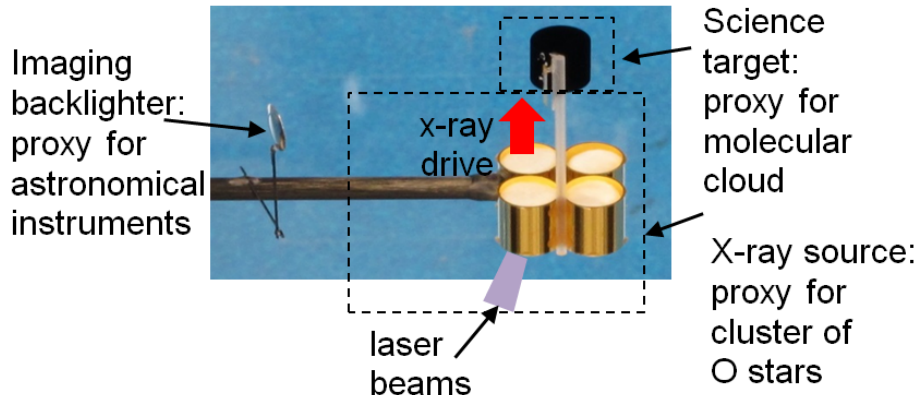


Figure 4: The long-duration, directional multi-hohlraum x-ray source. The source is four hollow cylindrical gold radiator cavities (hohlraums) 4 mm long by 3 mm in diameter. The insides of the hohlraums are irradiated by laser beams for 10-15 ns each, in series. The hohlraums reradiate the laser energy as 30-60 ns of x-rays, which is used to illuminate the science package. The science package representing a molecular cloud is stood off 5-8 mm from the source to see directional illumination. A separate ‘backlighter’ target is illuminated for a few ns by a different set of intense laser beams, and it reradiates hard x-rays used to radiograph the evolved target near the end of the main x-ray drive.

In the first set of NIF shots, the target was stood off 5-8 mm from the source. The science target consisted of a rough analog to the initial conditions Figure 2, featuring a dense structured clump at the surface of a background ‘cloud’. The background cloud was a 3 mm diameter by 5 mm long cylinder of 40 mg/cc C foam. The clump consisted of three discs of increasing diameter and decreasing density: a 0.6 mm diameter, 75 μm thick disc of 1 g/cc CH plastic; a 0.84 mm diameter, 105 μm thick disc of 475 mg/cc C foam; and a 1.4 mm diameter, 150 μm thick disc of 220 mg/cc C foam. The largest, lowest density disc was next to the background foam. The structured clump was designed to both shield the initial pillar and, later in time, feed material into an emerging cometary structure, the same as in Figure 2f. At the present time, a more ambitious target with a spherical, graded density graded clump embedded in the foam would be prohibitively expensive, although emerging 3D printing and deposition technologies could lower the cost in the future. Experimentally, the long foam cylinder used in these initial shots was simpler to deploy than a shorter foam, and corresponds to the ‘long cloud’ astrophysical simulations in Figure 2a-d.

The x-ray source was varied from shot to shot. The number of hohlraums used was increased from three on the first two shots, to four on the last two shots, while the laser energy delivered to each hohlraum was increased from 80 kJ to 120 kJ. The data in Figure 5 show that a longer duration drive gen-

erates a longer, more mature pillar. The standoff distance was also increased between shots, from 5 mm on the first shot to 8 mm on the final, 60 ns shot. Thus on the 60 ns shot, the shielding target was illuminated with lower x-ray flux due to the roughly inverse square law drop-off of intensity with distance, but was also driven with a larger total energy over a longer time. In addition, the dimensions and masses of the targets varied shot to shot from the design specification, accounting for some of the variations in the radiographed structure. While each of the radiographs happens to capture a well-developed pillar structure, iterative design was needed to find targets that generated a connected pillar. In the HYDRA simulations, shielding pillars usually ‘pinch off’ as the lateral shocks compress the background material converge onto the axis and push it downstream from the clump, resulting in a shocked clump separated from a shocked background cloud, the same as in our astrophysical simulations of shielding pillars. For the experiment, we chose layer dimensions and densities in the clump so that the shocks passing through the clump provided ablated and shock-released material to the pillar at later time as the shadowed background cloud material receded.

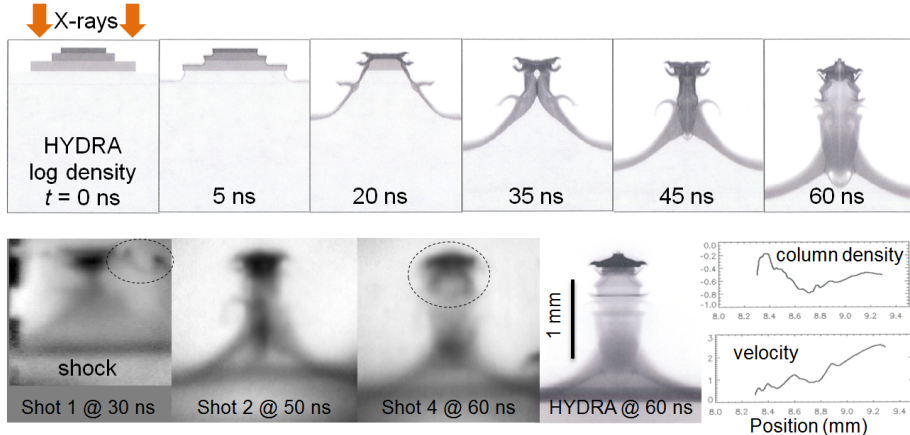


Figure 5: NIF shielding pillar design simulation and experimental data. Top: log density slices through the axis of the pillar from HYDRA simulations of the fourth NIF shot, which used four hohlraums to generate a 60 ns x-ray pulse. Bottom: Left three panels: Experimental radiographs from three of the four NIF shots. 2nd panel from right: simulated radiograph from a HYDRA simulation of the 60 ns shot. 1st and 3rd panels: The dashed ovals indicate apparent early development of cometary structures in addition to the mature ‘shielding’ pillar. Rightmost panels: Column density and velocity predicted by HYDRA for the 60 ns shot — to be compared with the column density and velocity profiles in Figure 2d.

Future Work

The NIF Discovery Science Committee has awarded our group two further NIF shots in 2017–2018 to focus on the cometary model of pillar formation. This work is already underway.

Presentations

- *Molecular Pillars in the Lab and in the Sky*, **Marc W. Pound**, Mark G. Wolfire, Jave O. Kane, David A. Martinez; 30 Years of Photodissociation Regions, July 2015 (<http://pdr30.strw.leidenuniv.nl>).
- *Dynamics of Molecular Clouds: Observations, Simulations, and NIF Experiments*, Jave O. Kane ; David A. Martinez ; **Marc W. Pound** ; Robert F. Heeter (LLNL); Alexis Casner (CEA); Roberto C. Mancini (U. Nevada-Reno);SPIE LASE 2015, February 12, 2015.
- *Molecular Pillars in the Lab and in the Sky* [revised], **Marc W. Pound**, Mark G. Wolfire, Jave O. Kane, David A. Martinez; HEDLA 2016
- *NIF Discovery Science: Eagle Nebula*, Jave O. Kane; **Marc W. Pound**, Mark G. Wolfire, David A. Martinez, HEDLA 2016
- *NIF Discovery Science 2017 Eagle Nebula*,**Marc W. Pound**, Jave O. Kane, M, David A, Martinez, presentation to NIF Discovery Science selection panel

Publications

- **Pound, M.W**, Wolfire, M.G., Grand, E., *Dense Gas in the Eagle Molecular Pillars*, in preparation for submittal to the Astrophysical Journal (detailed analysis of CARMA observations and photodissociation region modelling).
- Kane, J.O., Martinez, D.A., **Pound, M.W.**, Heeter, R.F., Casner, A., Villette, B.Mancini, R.C., *Dynamics of Molecular Clouds: Observations, Simulations, and NIF Experiments*;*Proc. SPIE 9345, High Power Lasers for Fusion Research III*, 93450C (February 26, 2015); doi:10.1117/12.2072369.
- Kane, J.O., **Pound, M.W.**, Martinez, D.A., Heeter, R.F., Casner, A., Villette, B. *Pillars of the Laboratory*,in preparation for submittal to the Physical Review D. (NIF shielding pillar shots)
- Kane, J.O., Martinez, D.A., **Pound, M.W.**, Heeter, R.F., Casner, A., Villette, B., Huntington, C. M., Mancini, R.C, *Laboratory Astrophysics with Long Duration Directional X-ray Sources*,in preparation for submittal to Physics of Plasmas Letters. (Omega EP LBS shots prototyping multi-hohlraum source and pillar targets.)
- Martinez, D.A., Kane, J.O., **Pound, M.W.**, Heeter, R.F., Casner, A., Villette, B., Mancini, R.C, *The long duration multi-hohlraum x-ray source*,in preparation for submittal to the Review of Scientific Instruments. (Multi-hohlraum source design, development, calibration and applications.)